

OBSERVATIONS ON THE LEGS OF TRIMALACONOTHRUS MANICULATUS  
FAIN & LAMBRECHTS, 1987 (ACARI, ORIBATIDA).  
PART 1. LARVA, LEG IV OF NYMPHS AND FUNDAMENTAL PHANEROTAXY.

BY Georges WAUTHY and Alex FAIN \*

TRIMALACONOTHRUS  
MANICULATUS  
EVOLUTION  
MALACONOTHRIDAE  
PHYLOGENY  
ONTOGENY  
MORPHOLOGY  
PARALLEL HOMOLOGY

SUMMARY : In this paper, the morphological diversity of legs (segments and phaneres) in *Trimalacothrus maniculatus* FAIN & LAMBRECHTS, 1987 is studied in larvae and leg IV of nymphs. Progressive and regressive evolutions shown by morphologic characteristics are surveyed to point out their possible relationships with various rules edicted by GRANDJEAN (e.g. the rule of parallel homology, rules of disjunction shown by phaneres, and so on) and discussed in the light of our present knowledge of the phylogeny in oribatids and Malaconothridae.

TRIMALACONOTHRUS  
MANICULATUS  
EVOLUTION  
MALACONOTHRIDAE  
PHYLOGENÈSE  
ONTOGENÈSE  
MORPHOLOGIE  
HOMOLOGIE PARALLÈLE

RÉSUMÉ : Dans cet article, nous abordons l'étude de la diversité morphologique que montrent les pattes (tant les articles que les phanères) chez une espèce de *Trimalacothrus* récemment décrite (*Trimalacothrus maniculatus* FAIN & LAMBRECHTS, 1987), par l'examen des larves et de la patte IV des nymphes. Une attention toute particulière est apportée aux évolutions progressives et régressives que montrent certains caractères morphologiques en relation avec diverses lois (comme la loi d'homologie parallèle, les règles de disjonction touchant certains phanères, etc.), et que nous discutons dans le cadre de nos connaissances actuelles de la phylogénie des Oribates et des Malaconothridae.

INTRODUCTION

To date, and despite the attempt by KNÜLLE (1957), we lack clear illustrations of progressive and regressive apomorphies shown by morphological characteristics of legs in Malaconothridae, and indicated by GRANDJEAN in several works (these are listed in the index of the "Oeuvres acarologiques complètes", vol. 7, p. 25 and p. 35).

Therefore, the information reported herein must be regarded as basic groundwork allowing a revision of Malaconothridae to be conducted in other

papers to come. However, changes of morphological characteristics during ontogeny and their variations between individuals were so important in the species studied that the purpose of the present article is first of all to report on the evolutionary phenomena shown by legs of the larva and leg IV of nymphs only. A second aim is to complete the description of *T. maniculatus* by FAIN & LAMBRECHTS (1987).

\* Institut Royal des Sciences Naturelles de Belgique, Entomologie, Rue Vautier 29, B-1040 Bruxelles (BELGIQUE).

## MATERIAL AND METHODS

All the specimens which underwent examination originated from aquaria located in Antwerp where the species was previously found. Standard observation and dissection technique in lactic acid (sometimes in distilled water) was used for the detailed study of 6 larvae, 5 protonymphs, 7 deutonymphs and 5 tritonymphs (i.e. 12 legs examined in detail among larvae, and 10, 14 and 10 in proto-, deuto- and tritonymphs, respectively), usually with heating of specimens in order to separate more easily the thick and so peculiar cerotegument covering the skeleton in Malaconothridae. Indeed, as pointed out by GRANDJEAN (1947 a, p. 167), this cerotegument is birefringent (the study of cerotegument in *T. maniculatus* is devoted to a separate paper).

Additional information was obtained using a scanning electronic microscope (microphotographies will be presented in the second part of the present work).

Our terminology is the one proposed by GRANDJEAN (see e.g. 1947 b, p. 5; and HAMMEN, 1980). However, we would like to indicate that, in order to compare legs I and II to legs III and IV (only to leg III in larva), each leg is described as though it extended perpendicular to the long axis of the animal's body. Therefore, each leg has a prime (anterior), double prime (posterior), dorsal and ventral face; but, due to the destruction of the plesiomorphic, perpendicular parallelism of legs (see GRANDJEAN, 1961, p. 211, for a discussion), the prime faces of legs I and II and the double prime ones in legs III and IV are closer to the long axis of the body (i.e. they are paraxial) than are the double prime and prime faces of legs I-II and legs III-IV, respectively (these faces are antiaxial; and, in lateral views shown by figures, only these faces of segments will be presented).

Except where otherwise stated, all the measurements related to the greatest dimensions (length, height or breadth) shown by the characteristic in question (a structure, a phanere or a segment). Finally, the main abbreviations we used are as follows: *Ad*, adult; *F*, femur; *G*, genu; *n1*, protonymph; *n2*, deutonymph; *n3*, tritonymph; *P*,

podosoma; *T*, tibia; *I*, *II*, *III* and *IV*, first, second, third and fourth leg, respectively.

## DESCRIPTION OF LEGS IN THE LARVA (Fig. 1)

Leg III is the longest of the three legs. Whereas legs I and II have approximately the same length and shape, leg I is, however, the broadest.

*Segments*

## Trochanter

In trochanters I and II, the dorsal face is the most developed whereas the ventral one is the least. Moreover, the dorsal face is strongly curved downward and narrowed forward so that the dorsal condyle of the joint trochanter/femur ( $\delta_d$ , Fig. 1A) is more distal than the ventral one ( $\delta_v$ , Fig. 1B). On the other hand, the antiaxial face is slightly depressed (*z* points the depression out in Figs 1A and B).

In trochanter III, the antiaxial face is the most developed whereas the paraxial one is the least. However, the curvature of the antiaxial face is less marked than the one shown by the dorsal side in legs I and II; nevertheless, its narrowed region supporting the antiaxial condyle of trochanter/femur articulation ( $\delta'$ , Fig. 1E) is well marked. The antiaxial face shows also a proximal bulge (*h*, Fig. 1E), the dorsal and ventral limits of which are quite worn away.

## Femur

Femora show two parts: a proximal one which is a short, relatively broad peduncle, and a distal one which is much longer and separated from the peduncle by a circular furrow (*sf*, Figs 1A, B and E). In fact, the longitudinal axis of the peduncle and the one of the distal part form an angle (the mean value of angles is around 19° in FI-II and 15° in FIII) in such a way that the femora are cambered in a paraxial direction. The length of the peduncle is reduced dorsally in femora I and II and antiaxially in femur III, i.e. facing the dorsal and prime condyles of trochanters, respectively. However, in the meantime, the depth of furrows *sf* is still substantial. In legs I and II, the ventral face of the

peduncle shows a ridge (*k* Figs 1A and B) which goes up a bit upon the antiaxial side of segments.

In front of furrow *sf*, the distal, elongate part of femora shows a shoulder (*e*) in the form of an uninterrupted, raised ring which is more marked (i.e. has the form of a true ridge; see optical section in Fig. 1B) facing the condyle *delta<sub>d</sub>* in legs I and II and *delta'* in leg III. In femora I and II, the seta *bv''* is located distally upon the shoulder (Fig. 1B). On the other hand, the localization of setae *dF* is not dorsal, but slightly paraxial in femora I and II, and a bit antiaxial in femur III; and, these displacements abide by the rule of "parallel homology" (hereafter RPH; see e.g. GRANDJEAN, 1961, p. 211, for a definition). In addition, in legs I and II, the dorsal face of the femora is slightly depressed paraxially (*z* Figs 1A and B).

Ventrally, in femora I and II, one can observe a groove (*r1*) which extends over both the lateral faces of the segment, but not dorsally. Paraxially, there is another groove (*r2*), the ventral extremity of which becomes indistinct at the level of two small pits located near the distal rim of the segment (in Fig. 1A and B, *f* is the antiaxial pit).

In femur III, distally, one observes a ventral swelling (*h* Fig. 1E) which extends a bit over both the lateral sides, and on which the seta *ev'* is inserted. The localization of *ev'* is thereby very distal on the segment (note that this seta is called *va'* by KNÜLLE, 1957, Fig. 3, p. 192). There is also a groove (*r*) and a ventral pit.

#### Genu

All the genera show two transverse carinas (note that these transverse carinas and all the ones observed elsewhere have a typical shape in so far as the distal side is always much more abrupt than the proximal one). One is dorsal (*kd*) and supports the solenidion *sigma* in genera I and II (the localization of solenidia is nearly axiodorsal on both segments). In front of this carina, the dorsal side of the genua shows a weak depression.

The second carina (*kv*) is ventral. In genu I, *kv* extends backward over both the lateral faces, in the form of slightly bulged swellings (*ar'* and *ar''* in Figs 1A and B) which support the setae *l'* and *l''* respectively. In genu II, only the antiaxial extension

*ar''* exists and supports the seta *l''* (Fig. 1C). In genu III (Figs 1D and E), the antiaxial extension *ar'* is much wider than the *ar''* one, and dorsally both the extensions join the dorsal carina (*kd*) in order to create a true raised ring (note that in several genera, the extension *ar''* was inconspicuous). Moreover, a small swelling (*h*) is developed behind *ar''*.

Finally, the localization of setae *dG* is not dorsal, but clearly paraxial in genera I and II, and antiaxial in genu III. These displacements are consistent with RPH.

#### Tibia

Tibiae I and II have four setae as in several other nothroids, and we used the notation proposed by GRANDJEAN (1940 a, p. 63). Both tibiae I and II have also a dorsal, transverse carina (*kd* Figs 1A, B and C) on which the solenidion *phi* is inserted and the tubercle of insertion of setae *dG* is partially located. These tubercles are well developed (but less marked, however, than the ones on which some gastronotic setae are). The dorsal carina goes down to both lateral faces of the segments (but not ventrally), and their paths depress these faces (a bit more antiaxially than paraxially). The consequence is that the lateral bulges appear relatively more marked in tarsi I and II than in tarsus III (in Fig. 1D, *h* is the paraxial bulge).

All the tibiae show: first, a little, dorsal ridge (*c*) joining the tubercle of seta *dG* to the one of solenidion *phi*; second, a ventral elevation (*h* Figs 1B, C and E) on which the setae *v'* are inserted, and the setae *li''* are in tibiae I and II.

#### Tarsus

Tarsi consist of two parts, the longitudinal axes of which bifurcate dorsoventrally. The torsion is achieved by the short, proximal part, the dorsal side of which is clearly bulging (the tarsi seem thereby to have a proximal "hump" indicated by *hu* in Figs 1B and E) whereas its ventral face is broadly furrowed (note that, though the hump is more marked in tarsus III than in both other tarsi, the angles of bifurcation are approximately the same, i.e. around 25° in tarsi I and II, and around 30° in tarsus III; see arrows *op* and *od* in Figs 1B and E).

All the lyrifissures (*ly*) are located on a small

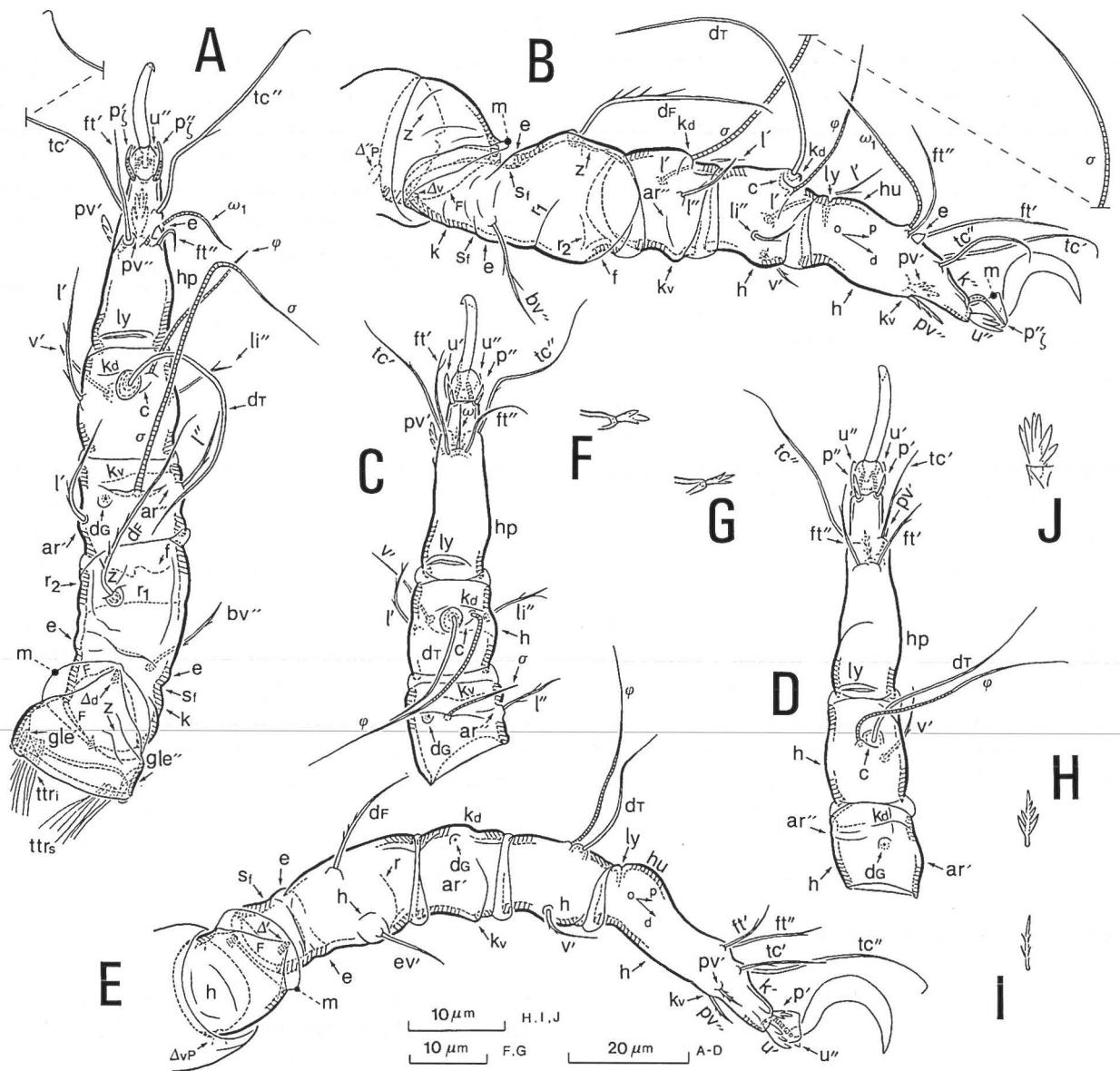


Fig. 1 : *Trimalaconothrus maniculatus* Fain & Lambrechts, Larva. — A : right leg I in dorsal view ; the solenidion *omega 1* is interrupted in order to let see the famulus *e* ; *ttri*, *ttrs*, superior and inferior tendons of trochanter ; the groove *r1* and the antiaxial pit *f* in femur, the carina *kv* in genu, and the seta *pv''* in tarsus are seen on the ventral face. — B : right leg I in lateral (antiaxial) view ; the paraxial vestige *dG*, difficult to be shown in this orientation, is not presented ; but, the dorsoparaxial depression *z* and the groove *r2* in femur, and the seta *pv'* in tarsus are presented. — C : right leg II in dorsal view ; genu, tibia, tarsus and apotele ; in genu, the tendon *tg* prolonged by the flexor muscle 8 in SHULTZ (1989, Fig. 6E, p. 23) is not presented ; the ventral carina *kv* in genu and the seta *pv''* (without notation) in tarsus are partially seen on the ventral face. — D : left leg III in dorsal view ; genu, tibia, tarsus and apotele ; the tendon *tg* is not presented ; the seta *pv''* (without notation) is seen on the ventral face of tarsus. — E : left leg III in lateral (antiaxial) view. — F : right leg II, distal part of dorsodistal ridge with the seta *p''* in lateral (antiaxial) view. — G : seta *p'* and ridge *k'* (partially) in the paraxial side of the tarsus shown in F. — H : right leg II, seta *pv''* in ventral view and flat shown. — I : left leg III, seta *pv''* seen as in H. — J : right leg II, ramose seta *pv''* shown *in situ* ; the inferior branches are on the right.

Note. In dorsal view, setae *u* cannot be outlined in details at the scale used ; thereby, only their visible contour is shown. Condylaphores, joint condyles and thickness of the skeleton (partially) are hatched.

Abbreviations. *ar* : lateral extension of the ventral carina of tibiae ; *c* : dorsal ridge of tibiae joining the tubercle of setae *dT* to the one of solenidia *phi* ; *delta* : condyle ; *e* : shoulder of femora or famulus of tarsus I ; *F* : proximoparaxial rim of femora ; *f* : pit ; *gle* : glenoid cavity ; *h* : swelling ; *hu* : dorsal hump of tarsi ; *k* : carina or ridge ; *m* : fold of a joint membrane ; *od* : arrow referring to the long axis of the distal, elongate part shown by tarsi ; *op* : *idem* for the proximal, short part ; *r* : groove ; *sf* : circumfemoral furrow ; *z* : depression.

proximal swelling, and show a paraxial basculation (i.e. prime in tarsi I-II, and double prime in tarsus III). Consequently, this displacement appears to be an evolution which is not consistent with RPH as is often the case (see e.g. GRANDJEAN, 1962 a, p. 96).

The three tarsi show a dorsal elevation on which setae *ft* are inserted. In tarsus I, the solenidion *omega 1* and famulus *e* are located on the elevation, and the insertion of solenidion *omega 1* is rather antiaxial (Fig. 1A). In tarsus II, the solenidion *omega* is inserted axiodorsally upon the elevation. Setae *tc* are likewise located on a dorsal elevation of the tarsi.

In front of this elevation, the dorsal face of the tarsi is flanked by two ridges which support distally the setae *p*. The ridges are more easily seen in the lateral orientation of tarsi than in the dorsal one (*k''* in Fig. 1B and *k'* in Fig. 1E are the paraxial ridges in tarsi I and III respectively; Figs 1F and G show also the distal extremity of both ridges in tarsus II).

In tarsi II and III, paired setae *p* and *u* show an antiaxial basculation (i.e. that both setae double prime in tarsus II and both setae prime in tarsus III have shifted downward with respect to the other setae); and, the degree of these basculations is quite similar to the one observed in some tarsi IV of nymphs (Fig. 3G).

On the other hand, the two sole, ventro-distal setae present on the tarsi are inserted on a small and slightly lateral carina (*kv* Figs 1B and E); and we used the notation (*pv*) for these setae (see annotation 1 at the end of the paper).

Finally, the ventral side of tarsi shows, behind the previous carina, a relatively elongate swelling (*h* Figs 1B and E) which extends a bit over both lateral faces of the segments. These extensions are more prominent antiaxially than paraxially. Note that: first, the greater prominence of extensions onto the paraxial side is not consistent with RPH; second, the swellings and their extensions seem to be the sole structures which are in the larva tentatively metahomologous to raised rings shown in leg IV of nymphs (more precisely the rings *ar1* and *ar2* shown in Figs 3E, F, J and I). The consequence is that the antiaxial prominence (*hp* Figs 1A, C and D) induces in all the tarsi a weak paraxial camber of the distal part of the segment.

## Joints

Where articulations of segments are concerned, a bicondylar, bidesmastic joint (i.e. a "pivot joint" sensu HAMMEN, 1977, p. 310; see also SHULTZ, 1989, p. 21) is observed in three cases: between the podosoma and the trochanter; between the trochanter and the femur; and, between the tarsus and the apotele.

On the other hand, the articulations femur/genu, genu/tibia and tibia/tarsus are monocondylar and monodesmastic (i.e. a transverse dorsal "hinge joint" and a flexor muscle). In these articulations, the hinge is relatively broad since its glenoid cavity is grooved within the dorsal rim of the proximal segment, along the dorsodistal part which is slightly depressed.

In legs I and II, the axis of rotation of the pivot joint podosoma/trochanter is nearly horizontal, i.e. almost perpendicular to the plane of pseudosymmetry. The paraxial condyle is, however, more dorsal than the antiaxial one (*delta''P* Fig. 1B) in such a way that the trochanter has an overall, dorso-ventral movement. Note that accordingly the two tendons of the trochanter must be noted *ttri* and *ttrs*, respectively.

The axis of rotation of the pivot joint trochanter/femur coincides nearly with the plane of pseudosymmetry (the dorsal condyle *delta<sub>d</sub>* is, however, more antiaxial than the ventral one *delta<sub>v</sub>*; see Figs 1A and B) in such a way that the femur mainly moves (more precisely rocks) laterally around the long axis of the leg. In leg III, an opposite lie of these axes is observed. Consequently, the overall movements of trochanter and femur III are definitely lateral and dorsoventral, respectively (the two tendons of trochanter III, not presented, must therefore be noted *ttr'* and *ttr''*).

Finally, due to the basculation of ungues (see below), the axes of rotation of the articulation tarsus/apotele do not coincide with the plane of pseudosymmetry; and besides, there is no posterior guidance for the tendon *ti* of apoteles.

## Phanerotaxy

Phaneres have the following formulae:  
*Setae*. I (0-2-[2+1v]-4-11-1); II (0-2-[1+1v]-4-10-

1); III (0-2-[1v]-2-10-1). *Solenidia*. I (1-1-1); II (1-1-1); III (0-1-0).

In these formulae, the vestige *v* is the one of setae *dG*. These setae do not emerge from their alveoli and appear as a spot. Nevertheless, their tubercles are relatively well marked.

The evolutions shown by other setae belong to two main categories depending on whether the differentiations have acted on their dimensions or on their forms as follows.

The first category refers to setae *dG* (see above) and *dT*. All the setae *dT* are long and tactile. They are vertically erected upon the segments, and then widely curved, more often than not, backward in legs I and II, and forward in leg III. Any *dT* is coupled with a solenidion.

The second category refers to setae *pv*, *tc*, *u* and *p* of tarsi :

— In legs I and II, the setae *pv'* and *pv''* (Fig. 1H) are ramose. Usually, there are four branches in *pv'I*, *pv''I* and *pv''II* whereas there are six branches in *pv'II* (Fig. 1J). At this point, two important remarks must be inferred. Firstly, whatever the notation of these setae may be (but assuming their metahomology; see annotation 1), the rule of "metameric reinforcement" is not respected (rule "c" in GRANDJEAN, 1959 a, p. 196). Indeed, in leg III, *pv'* as well as *pv''* (Fig. 1I) are not ramose but spiny (there are usually four spines, always short and thin). Second, assuming the present notation, the setae show in all three tarsi, at once, a clear basculation in a prime direction which accords with RPH, and a disjunction which does not. As a matter of fact, the disjunction is double prime in tarsus I whereas it is prime in both tarsi II and III (and more marked in III than in II). Consequently, the relative, forward displacement of *pv''* on tarsus I appears to be an apomorphy not consistent with the rule of prime disjunction (GRANDJEAN, 1960 a, p. 273) applied to paired setae *pv* in other oribatids (but, see the observations by TRAVÉ, 1971, p. 304, on tarsi I-II in *Mucronothrus nasalis*; and the marked exception to this rule shown by all the species of Hermanniellidae, as pointed out by GRANDJEAN, 1962 b, p. 659).

— Except for *tc'III*, the setae *tc* have a crozier-like tip. They are also twice curved. The first

curvature is directed laterally and upward whereas the second one is forward. The double curvature is more marked in setae *tc''* than in *tc'*, and in leg I than in legs II and III. In addition, because the course of *tc'III* is not curved but nearly rectilinear, only the morphological apomorphies shown by setae *tc''* are consistent with RPH. On the other hand, the paired setae *tc* in tarsus III show a weak antiaxial (prime) disjunction which apparently does not exist in tarsi I and II. This longitudinal shifting of seta *tc'III* appears then to be an apomorphy not consistent, at one and the same time, with the rule edicted by GRANDJEAN (1960 a, p. 273) indicating an usual double prime disjunction of setae *tc*, and with RPH (see annotation 2).

— The setae *u* are very characteristic. They are lanceolate, with a distal part both denticulate (there are usually five processes, including the median one) and folded in such a way that the concave, superior face of setae is applied to the membrane of tarsus/apotele articulation (therefore, the protecting role of setae *u* for this membrane cannot be denied). This differentiation of setae *u* is consistent with RPH.

— Except in leg I, where they are eupathidial, relatively long and clearly curved forward, the setae *p* are lanceolate, as are setae *u* (Figs 1F and G); but, they are shorter, less wide, and usually show three processes. Note that : first, the paraxial proral seta (i.e. *p'* in tarsus II, and *p''* in tarsus III) is always less robust than the antiaxial one; second, the processes of setae *p* in III are usually shorter than the ones shown in tarsus II.

Where the other phaneres are concerned, the setae *ft'* are thicker than *ft''* in tarsi I and II. Moreover, the setae *ft'* in legs I and II, and *ft''* in leg III are slightly curved forward, whereas *ft'I*, *ft''II* and *ft'III* are usually curved backward. On the other hand, the famulus (*e*) is a short, cuneiform seta (Figs 1A and B). Among the remaining setae, the dorsal ones (*dFI*; *dFII*), the paralateral ones (*l'*) and the seta *v'III* are more curved forward than the others (note that, at the bottom, the course of setae *dF* in legs I and II is directed paraxially and upward). In addition, all these setae are barbellate; but, the barbels are variable in number (the most

barbellate seta appears to be *dFI*, and its barbels are also the most robust), always thin and, usually, scarcely discernible.

The paired setae *l* of genu I show concomitantly an antiaxial (double prime) disjunction and a basculation (i.e. an isotrope shifting of the seta *l''GI*). Note that the disjunction in question is consistent with the rule edicted by GRANDJEAN (1960 a, p. 273). Where setae *l* and *v* of genua and tibiae are concerned (i.e. *l'GI*, *l'TI-II*, *l''GI-II* and *v'TI-III*), an important conclusion must be inferred : the localization of these setae is not typically the ones observed in primitive conditions (i.e. latero-dorsal in *l* setae and lateroventral in *v* setae as e.g. in *Palaearcarus appalachicus* ; see GRANDJEAN, 1940 b, p. 33). Consequently, one can assume that all these phaneres have shifted a bit downward (and relatively more in setae *v* than in setae *l*) ; and, these displacements are apomorphies consistent with RPH.

The ungues are relatively robust. They show a slight basculation which is paraxial in leg I and

antiaxial in legs II and III (i.e. double prime in leg II and prime in leg III). Using SEM one can observe : first, very minute and low ridges located laterally on the proximal part of ungues (the most elevated ridges were less than 0.30  $\mu\text{m}$  high) ; second, three or four very small barbels located dorsoproximally on each side. Distally, the inferior border shows a small swell with the result that the tip of ungues appears to be nicked (more in unguis III than in both the others). Note that this nick is not homologous to the one shown by ungues (*ol*) in several Circumdehiscent oribatids (see GRANDJEAN, 1960 b, p. 101).

Solenidia are either piliform (*sigmaII* ; *omegaII*) or tactile (*sigmaI* ; *phi* in I, II and III ; *omegaI*). This means that no "primitive" solenidion exists (GRANDJEAN, 1961, p. 222). *OmegaI*, *phiI* and *phiII* are vertically erected on their segment whereas the other solenidia escape forward, following an acute, more or less marked angle.

Figure 2 attempts to show a schematic survey of the main evolutionary phenomena brought to light

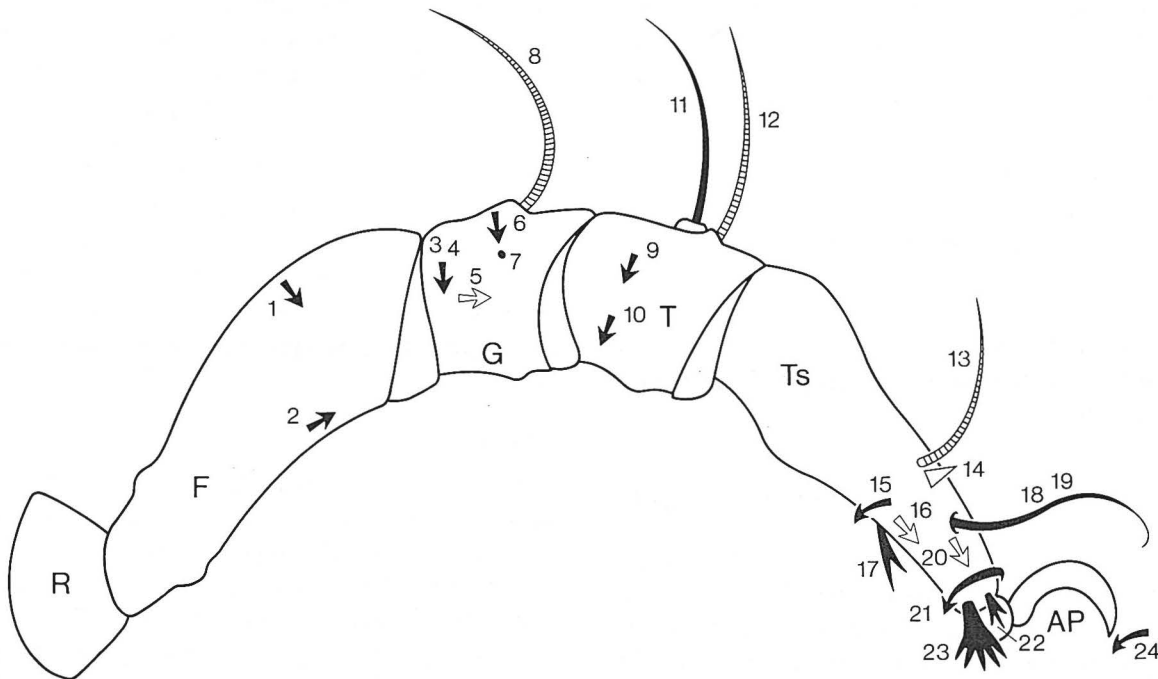


Fig. 2 : Schematic representation of the 24 main apomorphies shown by phaneres in the larva of *Trimalaconothrus maniculatus* Fain & Lambrechts. See the text for definitions of evolutionary phenomena outlined.

Note. Open arrows refer to phenomena of disjunctions.  
Abbreviations. *R* : trochanter ; *Ts* : tarsus ; *AP* : apotele.

by our present study on the phaneres of larvae in *T. maniculatus*. The phenomena could be classified into two groups according to the fact that either they abide by RPH (an asterisk marks such apomorphies) or they do not square with this rule. There are, from femora to apoteles : (1) Weak lateral shifting of setae *dF* onto the prime face of femora (\*). (2) Advance of the seta *ev'* in femur III. (3) Descent of the seta *l'* in genu I. (4) Descent of the seta *l''* in genua I-II. (5) Double prime disjunction of setae (*l*) in genu I. (6) Lateral shifting of setae *dG* onto the prime face of genua (\*). (7) Drastic shortening of all the setae *dG*. (8) Lengthening of solenidion *sigma* in I. (9) Descent of the seta *l'* in tibiae I-II. (10) Descent of the seta *v'* in all the tibiae (\*). (11) Lengthening of setae *dT* and hypertrophy of their tubercle. (12) Lengthening of solenidion *phi* in all the tibiae. (13) Lengthening of solenidion *omega* in tarsus I. (14) Shape of famulus *e*. (15) Prime bascultation of setae (*pv*) in all the tarsi (\*) (see also annotation 1). (16) Disjunction of setae (*pv*), double prime in I and prime in II-III. (17) Shape of setae (*pv*) in tarsi I-II. (18) Lengthening and curvatures of setae *tc''* (\*). (19) Lengthening and curvatures of setae *tc'* in tarsi I-II. (20) Weak, prime disjunction of setae (*tc*) in tarsus III. (21) Bascultation of setae (*p*) and (*u*) in tarsi II-III. (22) Shape of setae (*p*) in tarsi II-III. (23) Shape of setae (*u*) in all the tarsi (\*). (24) Bascultation of ungues.

To complete the list of previous apomorphies, three important characteristics should also be stated : the bascultation of lyrifissures ; a clear tendency shown by proximal setae of tarsi to have moved forward ; and, the weak number of fundamental setae on tarsi.

#### DESCRIPTION OF LEG IV OF DEUTONYMPH (Fig. 3)

First, because the fundamental setae of leg IV are observed in n2, we describe in detail the leg IV of this instar. Second, by comparison, we study the changes that morphological characteristics of leg IV show in the two other instars. Third, the phaneres are investigated.

#### Trochanter

The antiaxial face of trochanter IV, which is much more developed than the paraxial one, is weakly bulging. In fact, there are two raised rings (a proximal one *ar1*, and a distal one *ar2*) which depress the antiaxial face. The anterior ring is broader than the posterior one ; but, both rings have approximately the same height. The two rings likewise depress the dorsal and ventral sides (but, a bit less strongly than antiaxially). In addition, ventrally, their path creates two clear furrows ; and, the rings meet paraxially in order to furrow deeply the paraxial face.

On the other hand, the trochanter shows two ridges. The distal one (*ka*) escapes ventroantiaxially from the ring *ar2*, and goes up a bit to the antiaxial side. The proximal ridge (*kp*) does not seem to be circular, but does not persist upon the paraxial side.

The axis of rotation of the pivot podosoma/trochanter as well as the one of the pivot trochanter/femur are closer to the horizontal plane of the leg than the plane of pseudosymmetry. However, the prime condyle of the trochanter is more dorsal than the double prime one (*delta''* Figs 3A and B). This latter is definitely more proximal ; and, the prime condyle of the podosoma (not presented, but *gle'* and *gle''* are the glenoid cavities of the pivot podosoma/trochanter ; Figs 3A and B) is more ventral than the double prime one.

Consequently, the overall movements of both trochanter and femur are dorso-ventral ; but, in a high position, it is likely that the trochanter deviates from the body whereas the femur comes near the body.

#### Femur

Femur IV is paraxially cambered ; but, the camber is clearly less sharp than the one shown by femora of larvae (the angle between the longitudinal axis of peduncle and the one of the distal part is around 5° ; see arrows *op* and *od* in Fig. 3A).

Ventrally, the furrow *sf* separating the peduncle from the distal part is poorly marked (Fig. 3B). Behind *sf*, the peduncle shows a ridge (*k*) which has a path not transverse but backwardly oblique (it is seen on the ventral face in Fig. 3A). Where the

other faces of the femur are concerned, the peduncle is nearly inconspicuous antiaxially whereas the depth of the furrow *sf* is much more marked antiaxially than paraxially, and still less dorsally than paraxially.

The shoulder (*e*) is a circular, uninterrupted raised ring which is both less high in the dorsal face and less broad in the ventral face than in the other faces. The dorsal side of the distal part of femur shows an elongate, paraxial depression (*zd*; the optical section 3C shows its depth and width at the level of seta *dFn2*). Proximally, the depression joins the shoulder. Distally, it flows into the dorsodistal, depressed part of femur, the border of which hinges with the genu.

All the faces of the distal part of the femur show a great number of small structures developed in the form of intricate swellings and hollows. The precise shapes and limits of these structures are quite difficult to study. Nevertheless, in the lateral orientation of the segment, six or seven structures can be observed ventrally (Fig. 3B). Swellings and hollows are more marked on the paraxial and ventral sides than on both the other faces (they don't seem, however, to exist dorsodistally).

Therefore, though the small structures showed little, individual variation, we could identify three swellings we define as follows (they are dotted in Fig. 3B) : *hv* is built paraxially and in front of the shoulder ; *he* is dorsoparaxial and joins proximally the dorsal part of the shoulder ; *ha* is more distal than the previous swelling, and goes up a bit upwards in order to make way upon the dorsoparaxial depression *zd*.

#### Genu

The dorsal face of genu IV shows a transverse carina on which the seta *dGn2* is inserted (note that the localization of this seta is not axiodorsal, but rather antiaxial). Paraxially, the dorsal face is depressed (*zd* Fig. 3B). This depression extends forwards in order to join the distodorsal part of genu, the border of which hinges with the tibia. There are also two raised rings (in Figs 3A and B, *ar1* is the proximal one, and *ar2* is the distal one) less high, however, than the transverse carina.

The three other faces of the genu are bulging ;

but, ventrally, the bulge exists only distally. In fact, the ventral face shows a proximal depression (*zv*) which extends a bit ventroantiaxially. As shown in Fig. 3A, the long axis of *zv* is oblique ; but, in the lateral orientation of Fig. 3B, *zv* is barely discernible.

Both the rings *ar1* and *ar2* as well as the dorsal carina go down to the paraxial and antiaxial faces. Making their path antiaxially, the ring *ar2* and the extension of the dorsal carina depress the antiaxial face with the result that the antiaxial bulge appears to be divided into two in the dorsal orientation shown by Fig. 3A. Note that : first, in 1/14 genua studied it was not ; second, the distal ring *ar2* was sometimes less marked than in Fig. 3A.

The ring *ar2* curves backwards in order to join the extension of the dorsal carina. Entering into the depression *zv*, both the extensions weaken drastically (only the extension of the dorsal carina keeps some consistency). Paraxially, the distal ring *ar2* curves relatively more strongly than antiaxially.

The ring *ar1* curves a bit backwards while it depresses the paraxial face much more, however, than both the ring *ar2* and the extension of the dorsal carina do (as shown in Fig. 3A, the paraxial depression due to *ar1* extends even up to the proximal rim of the segment) ; and, the ring *ar1* weakens substantially upon the ventral side.

#### Tibia

Dorsally, tibia IV shows : a proximal ring (*ar1* Figs 3F) which is poorly raised and depresses weakly the dorsoproximal, bulging part of the segment with the result that the tibia seems to have a hump (*hu* in Fig. 3E) ; a transverse carina (*kd* Figs 3E) which bears the seta *dTn2* ; and, a second, raised ring (*ar2*) located upon the dorsodistal, slightly rounded part of tibia.

The path shown by the proximal ring *ar1* on both the lateral faces is forwardly oblique (more paraxially than antiaxially). The ring is weakly discernible in the antiaxial orientation of the segment ; but, Fig. 3E allows its precise, lateral localizations to be inferred. Ventrally, *ar1* keeps at short distance from the extension of the dorsal carina whereas, paraxially, both the extensions meet together (in some cases, a small groove joined

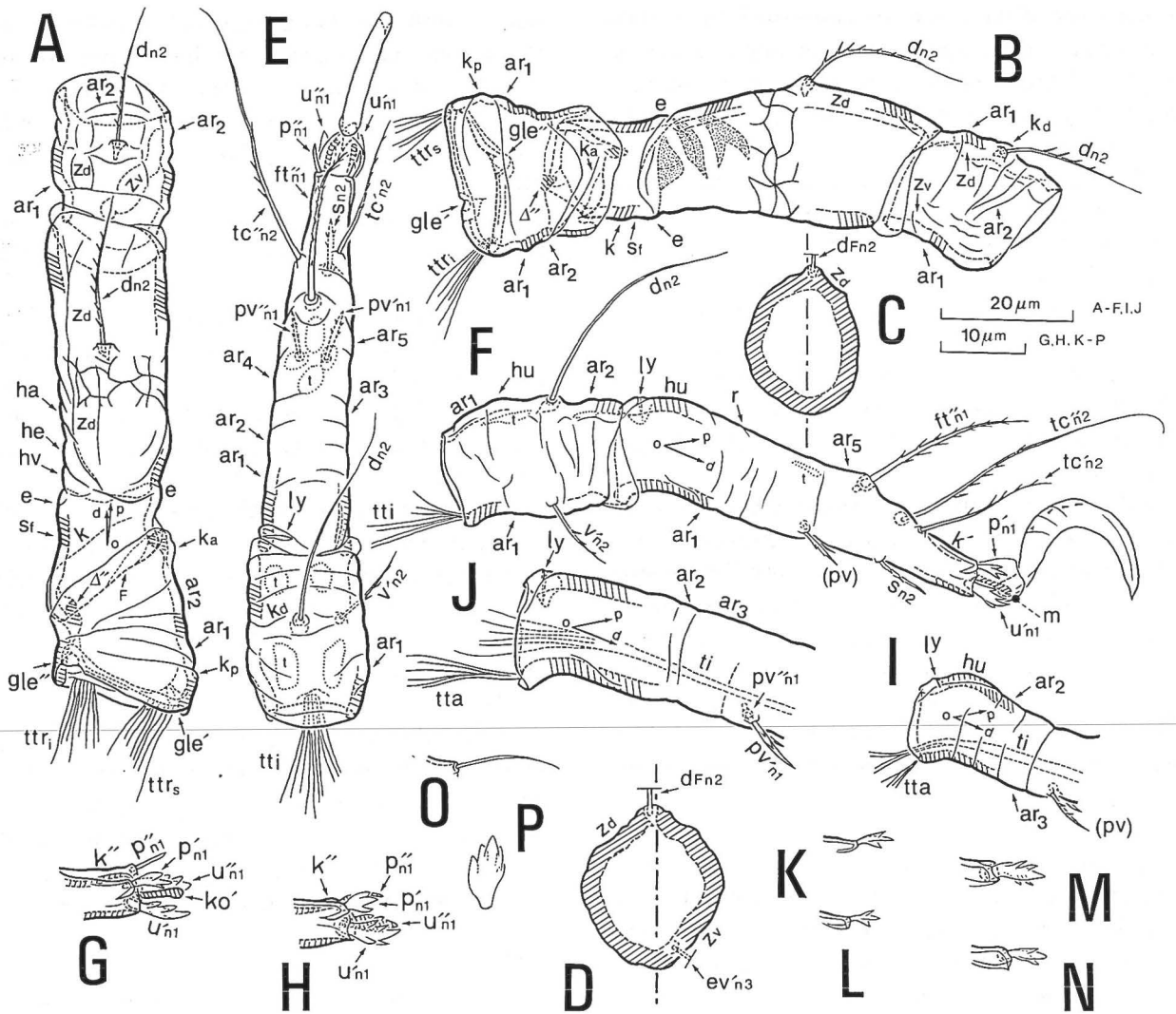


Fig. 3 : *Trimalaconothrus maniculatus* Fain & Lambrechts, left leg IV. — A : deutonymph, dorsal view ; trochanter, femur and genu ; the small swellings and hollows of femur are partially shown ; proximally, only the dorsal rim of femur (F) is indicated ; *ttrs*, *ttri*, superior and inferior tendons of trochanter. — B : deutonymph, lateral (antiaxial) view ; trochanter, femur and genu ; the small swellings and hollows of femur are presented partially ; stippled designs refer to the swellings *hv*, *he* and *ha* which, as well as depressions *zd*, are seen on the paraxial face. — C : optical section across the femur of deutonymph at the level of seta *dFn2* (the proximal part of which is only presented) ; the paraxial face is on the right, and the line with strokes and points refer to the plane of pseudosymmetry. — D : *idem*, in one tritonymph ; the paraxial face is on the left ; the seta *ev'n3* which is in front of the section is stippled ; only the proximal part of setae is presented. — E : deutonymph, dorsal view ; tibia, tarsus and apotele ; *tti*, tendon of tibia prolonged by muscles 6 and 7 in SHULTZ (1989, Fig. 6E, p. 23). — F : deutonymph, lateral (antiaxial) view ; tibia, tarsus and apotele. — G : deutonymph, lateral (antiaxial) view of the distal extremity of tarsus in order to show the basculation of paired setae (*p*) and (*u*) ; only the antiaxial condylophore *ko'* is presented. — H : *idem*, but no basculation is observed and no condylophore is presented. — I : protonymph, lateral (antiaxial) view of the proximal extremity of tarsus ; *ti*, inferior tendon of apotele. — J : *idem*, in tritonymph ; *tta*, tendon of tarsus prolonged by the flexor muscle 3 in SHULTZ (1989, Fig. 2E, p. 13). — K : protonymph, distal part of the dorsodistal ridge of tarsus with the seta *p'n1* in lateral (antiaxial) view. — L : *idem* with the seta *p'n1* in lateral (paraxial) view. — M : tritonymph, *idem* with the seta *p'n1* in lateral (antiaxial) view. — N : *idem* with the seta *p'n1* in lateral (paraxial) view. — O : abnormal seta *p'n1* in left leg IV of one protonymph, in lateral (antiaxial) view. — P : seta *u'n1* separated from the tarsus of a tritonymph and flat shown.

Note. Condylophores, joint condyles and thickness of the skeleton (partially) are hatched.

Abbreviations. *ar* : raised ring ; *delta* : condyle ; *e* : shoulder of femur ; *gle* : glenoid cavity ; *h* : swelling ; *hu* : dorsal hump of tibiae and tarsi ; *k* : ridge or carina ; *m* : fold of a joint membrane ; *op* : arrow referring to the long axis of the proximal, short part shown by femora and tarsi ; *od* : *idem* for the distal, elongate part of these segments ; *r* : groove ; *sf* : circumfemoral furrow ; *t* : prints of muscular insertion ; *z* : depression.

both the extensions ventrally). Moreover, behind *ar1*, the paraxial side of the segment is slightly depressed.

The ring *ar2* and the dorsal carina extend also over both the lateral faces which are more depressed by these extensions than by the one of *ar1*. In its lateral paths, the extension of *ar2* curves backward whereas the one of the dorsal carina curves only in the antiaxial face in order to proceed in front of the seta *v'n2*.

Finally, the seta *v'n2* is inserted on a ventral swelling which extends a bit antiaxially. The extensions of both *ar1* and the dorsal carina do not depress this swelling; but, on the contrary, they smooth substantially when they reach this structure.

#### Tarsus

Tarsus IV is the segment, the overall shape of which is the most similar to the one shown by tarsi of the larva. Indeed, one can observe: a proximal, dorsoventral torsion of the segment; a small swelling which supports the lyrifissure *ly*; a proximal hump *hu* (but, only in *n1* and *n2* as shown in Figs 3F and I); a distal, paraxial camber (but, only in *n1* and *n3*); two dorsodistal elevations (only one in *n1*); two distal ridges supporting the setae *p*; and, a ventral carina (on which, however, the seta *sn2* is inserted). Nevertheless, where details are investigated, these features are quite different.

The longitudinal axes of both the proximal, dorsally bulging part and the distal, elongate part of the tarsus bifurcate dorsoventrally at an angle of around 30° (the mean value was precisely 31°). Proximally, the distal part of tarsus IV shows five raised rings (*ar1-5*, Fig. 3E). Dorsally, the rings are usually poorly distinct except between *ar2* and *ar3* (in Fig. 3F, *r* is their dorsal parting groove). Ventrally, their limits are more conspicuous (especially, the limit between *ar4* and *ar5*); but, the parting between *ar5* and the remainder of tarsus is quite inconspicuous.

The ring *ar4* supports ventrodistally the paired setae (*pv*). Dorsally, the ring *ar5* shows the elevation on which the seta *ft'n1* is inserted (the localization of this seta is not axiodorsal, but still slightly paraxial). In addition, as the paraxial side

of *ar5* is more developed than the antiaxial one, this ring is the cause of the antiaxial camber shown by the distal part of the tarsus (Fig. 3E).

In front of the ring *ar5*, there is a second dorsal elevation, less marked, however, than the previous one. The seta *tc'n2* is inserted on this elevation whereas the seta *tc'n2* is usually not (the localization of this seta seemed as often as not to be just a bit in front of the elevation).

This means that the paired setae (*tc*) show an antiaxial (prime) disjunction as is observed in tarsus III of larvae; but, much more distinct. Such a disjunction does not accord with the rule of double prime disjunction commonly shown by setae *tc* (GRANDJEAN, 1960 a, p. 273; see annotation 2).

In 3/14 tarsi studied, the paired setae *p* and *u* showed a clear, antiaxial bascultation (Fig. 3G). However, the bascultation was either non-existent (Fig. 3H) or very weakly marked in all the other cases. On the other hand, the localization of the seta *sn2* upon the ventral, transverse carina is not axial, but rather antiaxial (note also that the path of the carina is a bit oblique antiaxially).

#### Apotele

What was most striking in the articulation tarsus/apotele is the relative robustness of the condylophores (e.g. *ko'* Fig. 3G) when compared with the ones of larvae.

The tendon *ti* of the apotele has no posterior guidance and the muscle of the tendon *ts* (i.e. the levator muscle 1 in SHULTZ, 1989, Fig. 2E, p. 13) has a clear, dorsal implantation on the inner side of both the rings *ar4* and *ar5* (*t* Fig. 3E). Note that, as usual, the implantation of the depressor muscle prolonging the tendon *ts* is dorsal, on the inner side of the tibia; and, this muscle is *n.2* in Fig. 2E by SHULTZ (*loc. cit.*).

#### LEG IV OF OTHER NYMPHS

The main changes shown by leg IV in *n1* and *n3* are as follows.

##### Trochanter

In *n1*, the distal ring *ar2* is weakly marked, except on the dorsal face where it is approximately as broad as the proximal ring *ar1*. This latter is well

developed on all faces of the segment ; but, its path furrows the ventral side much less intensively than in n2. The ridges *ka* and *kp* do not seem to exist.

In n3, both the rings are quite inconspicuous on the antiaxial face where they are likewise nearer than in n2. Consequently, they create a small swelling in the middle of this face. The ridge *kp* is less marked dorsally than in n2. The ridge *ka* is conspicuous only in the ventral side where it supports the seta *v'n3* (note that the localization of seta *v'n3* is almost axioventral ; see below).

#### Femur

In n1, what was most noticeable is the weak, relative lengthening of the segment. Indeed, the height-length ratio decreases substantially between n1 and n2 (in n1, this ratio is around 0.43 whereas it is around 0.36 and 0.33 in n2 and n3, respectively).

Ventrally, the convexity of the peduncle due to the ridge *k* is more marked in n1 than in both the other instars. In n3, paraxially, the furrow *sf* is divided into two by a small ridge ; in addition, its dorsal depth is greater than in n2.

Where the distal, elongate part of the femur is concerned, the shoulder is a bit more marked dorsally in n1, and a bit broader ventrally in n3 than in n2. The seta *dFn2* is located less distally in n3 than in n2. Moreover, the number of small swellings and hollows seem to be lower in n1 and greater in n3 than in n2 (in the lateral orientation of the segment, one can count ventrally up to five or six small structures in n1, and eight or more in n3).

On the other hand, in n1, the most distal swelling is more marked and closer to the rim of femur than in n2 ; and, two hollows located approximately in the middle of the ventral face are easily discernible. In n3, the swelling *hv* was sometimes smaller and less marked paraxially than in n2. Finally, one of the most distoventral swellings supports the seta *ev'n3* (the localization of this seta is, however, antiaxial). This swelling is located within an elongated depression (*zv*) which furrows ventroantiaxially the distal part of femur along approximately half of its length (*zv* is thereby less long than *zd*). The optical section 3D allows their respective vastness to be compared in n3.

#### Genu

The shape of genu IV is more different from the one shown by n2, in n1 than in n3.

In n1, the dorsoparaxial depression (*zd*) and the ventroantiaxial one (*zv*) are not present. So is the proximal ring *ar1* (in fact, one observe a circular groove in lieu of this ring). Dorsally, the transverse carina is more proximal than in n2 ; and, the distal ring *ar2* is more distal and more marked than in n2. Laterally and ventrally, the extensions of both *ar2* and the dorsal carina as well as the posterior groove are easily discernible.

On the antiaxial face, first, the extension of *ar2* does not curve. Second, the depression due to the extension of the dorsal carina is more marked than both the one created by the extension of the distal ring *ar2* and its homologue shown in n2 (consequently, the two bulges of the antiaxial face are always clearly marked in the dorsal orientation of the segment). Third, there is an oblique groove which joins both the previous extensions.

On the ventral face, the ring *ar2* depresses the skeleton more strongly than the extension of the dorsal carina does, with the result that one can observe two ventral swellings instead of one as in n2.

Finally, the paraxial face of the segment is less bulging in n1 than in n2, and there is no proximal depression as in n2.

In n3, dorsally, the distal ring *ar2* is more marked and more distal than in n2 whereas it is quite the reverse for the proximal ring *ar1* and the dorsal, transverse carina. Moreover, this carina is more distal (and, consequently, the localization of seta *dGn2*).

On the other hand, the lateral and ventral bulges are poorly developed. So are the lateral extensions of both the rings and the dorsal carina as well as the depressions they create respectively (only the lateral extensions of the dorsal carina depress a bit the skeleton) with the result that, in n3, the genu shows two antiaxial swellings fairly less marked than in n1.

Finally, the cylindrical feature of the segment in n3 is bolder than in n1 (in n3, the length-height ratio is around 0.78 whereas it is around 0.96 in

n1); but, the cylindrical feature is not significantly different between n2 and n3 (the ratio in question is around 0.76 in n2).

#### Tibia

The tibia is more globular in n1 than in n2, and significantly less in n3 (the height-length ratio is around 0.78, 0.67 and 0.60 in n1, n2 and n3, respectively).

The dorsoproximal hump is barely marked in n3 whereas, in n1, it is relatively more developed than in n2. In addition, the dorsal, transverse carina is more distal in n3 than in n2. Consequently, in n3, not only the seta *dTn2* is more distal but also the depressed, dorsodistal part of the segment is narrower. In n1 as well in n3, the rings *ar1* and *ar2* are less marked than in n2; and, the ventral swelling is more distal in n1 than in n2 whereas its relative position in n3 is approximately the one of n2.

Where the lateral and ventral extensions of the two rings and the dorsal carina are concerned, one observes that :

In n1, the extension of the distal ring *ar2* on both lateral faces is poorly curved backwards. It results from this that *ar2* keeps everywhere at a short distance from the extension of the dorsal carina. Ventrally, the extension of both the rings and the one of the dorsal carina are weakly marked.

In n3, first, the paraxial extension of the distal ring *ar2* and the one of the dorsal carina are relatively closer than in n2. Second, the ventral swelling is depressed by both the previous extensions. Third, the extension of the proximal ring *ar1* is much less oblique than in n2 and, thereby, more proximal ventrally on the segment.

#### Tarsus

The value of the angle of dorsoventral torsion is a bit more marked in n1 than in n3 since the mean value we measured in n1 was 35° whereas it was 30° in n3 (compare Fig. 3I with Fig. 3J).

The cylindrical feature of the distal, elongated part of tarsus IV is significantly less marked in n1 than in both the other nymphs. Indeed, in n1, the height-length ratio was around 0.27 whereas it was around 0.23 and 0.21 in n2 and n3, respectively

(note that we used in these ratios the height of tarsi measured at the level of the ring *ar1*).

In n1, the lyrifissure *ly* has not shifted paraxially (Fig. 3I) whereas, in n3, no dorsoproximal hump is developed (Fig. 3J). Such changes during ontogeny appear then to be unambiguous examples of a rule, the accuracy of which was time and again checked by GRANDJEAN (see e.g. 1964 a, p. 385), i.e. the ontogenetic independence of progressive as well as regressive evolutions ("each level of ontogeny has its own phylogeny").

Indeed, both the basculation of *ly* and the creating of a hump are morphological evolutions which are achieved (apomorphic state) or not achieved (plesiomorphic state) at a given level of ontogeny without their necessary enforcement on another, preceding or following instar. This means that, in *T. maniculatus* : first, the lyrifissure was (and has probably ever been) dorsal in the ancestors of present protonymphs; second, the ancestors of present tritonymphs had no proximal hump upon the tarsus of their legs IV. In other words, the plesiomorphic state of both evolutions is still observed today in both instars.

On the other hand, the basculation of paired setae (*p*) and (*u*) is an evolution, the apomorphic state of which seems to be definitely gained by n1 (at least, in the population studied). On the contrary, in 4/10 tarsi studied in n3, the plesiomorphic state (no or a weak basculation) was observed yet (note that no individual showed this state simultaneously on both its tarsi).

Finally, we must also indicate that :

In n3, the ring *ar2* is very narrow, and clearly furrows the segment (Fig. 3J).

In n1 and in n3, the distal camber of tarsus IV is just the opposite of the one shown in n2 since it is in a paraxial direction; but, the camber is due to the ring *ar4* in n1, and to the ring *ar5* in n3. More precisely, one observes in the rings in question a lengthening of the antiaxial side at the expense of the paraxial one.

In n1, there is no dorsal elevation homologous to the one supporting the seta *tc"n2* in n2 and n3.

In n3, the paired setae (*pv*) show a weak, antiaxial (prime) disjunction (note that this disjunction is more marked in Ad).

PHANEROTAXY

Phaneres of leg IV have the following formulas :

*Setae*. n1 (0-0-0-0-7-1) ; n2 (0-1-1-2-10-1) ; n3 (1-2-1-2-10-1).

*Solenidia*. n1, n2, n3 (0-0-0).

Setae of tarsus

The formula of n1 is the most common observed in oribatids (GRANDJEAN, 1933, p. 38 ; 1946, p. 299), and is due to the strong inhibition which acts in this instar upon the setae of leg IV in the form of a numerical, accelerated regression, and against which only seven setae are able to hold out, i.e.  $ft''n1$ , ( $p$ ), ( $u$ ) and ( $pv$ ).

The seta  $ft''n1$  is the most robust of dorsoposterior phaneres developed in tarsus IV. Proximally, it escapes from the segment at a relatively sharp, acute angle. Distally, it is more curved forward and in an antiaxial direction in n1 than in n2 (Fig. 3F). This illustrates the fact that, as usually, the above indicated inhibition does not act upon the shape and size of setae remaining on tarsus IV (see GRANDJEAN, 1946, p. 306 for a discussion). In n3, however, its course is usually the one shown in n2 (in some tarsi, it was more curved forward).

The seta  $tc'n2$  is the longest phanere shown in tarsus IV. Within a short distance of its base, the seta is rather curved upwards (Fig. 3F). Consequently, it does not show a proximal curvature in a paraxial direction as e.g. its metahomologue in leg III of the larva. More distally, it shows a weak curvature at one and the same time forward and paraxially ; and, its tip is crooked. Note that, in some tarsi studied in n2 and n3, the distal curvature in a forward direction was inconspicuous, and the course of the seta was nearly rectilinear (nevertheless, distally, the seta deviated, as usual, from the segment).

The seta  $tc'n2$  has a course similar to the one of the previous seta. However, its very tapered tip is not crozier-like, but shows a more or less straight curvature usually in a forward direction (in fact, varied directions were observed in n2 as well in n3). In addition, the seta seems relatively more robust, and its tip relatively less curved in n3 than in n2.

All the dorsoposterior setae are barbellate (two rows of barbels are observed in  $ft''n1$ ), and the number of barbels increases during ontogeny (e.g., in n2,  $tc'n2$  shows 5,6 barbels whereas 8-10 are counted in n3). In n2 and n3, the length of  $tc'n2$  is usually lower than the one of  $ft''n1$  ; but, in 1/14 tarsi studied in n2,  $tc'n2$  was clearly longer (and also strongly curved backward).

In n2, the shape of paired setae  $p$  is very different (Figs 3G and H) :

The seta  $p'n1$  is a short, lanceolate phanere quite similar to the ones we observe in tarsi II and III of the larva. Usually, there are three processes, and the median one is, as often as not, the longest.

The seta  $p''n1$  is a short, spine-like phanere which, usually, is smooth and comes to an end in the form of a more or less thick point.

In n1 and n3, both the setae  $p$  are short and lanceolate ; and, the seta  $p'n1$  is always more robust than the seta  $p''n1$  (and even, in n3, shows significantly more processes, i.e. usually five ; compare Fig. 3K to Fig. 3L and Fig. 3M to Fig. 3N, respectively).

Consequently, the seta  $p''n1$  shows, during ontogeny, changes of shape more abrupt and more drastic (i.e. lanceolate in n1 ; spine-like in n2 ; and, once again lanceolate in n3) than the ones of seta  $p'n1$ . This appears to be a second clear illustration of the rule of ontophylogenetic independence of evolutions we discussed above.

In 1/10 tarsi studied in n1, the seta  $p'n1$  was a relatively long and thin phanere (Fig. 3O) having a form that we could presumably regard as the plesiomorphic form of setae  $p$  (at least, in the ancestors of *T. maniculatus*).

We may then suppose that three morphological progressions should have acted upon setae  $p$  on and after this plesiomorphic state : first, a substantial shortening (as e.g. the one shown by  $p''n1$  in n2 ; see Figs 3G and H) ; second, a flattening along the longitudinal axis of setae ; and, third, a spreading out of extensions.

In addition, the development of extensions was probably as follows in the process of phyletic time T : firstly, two extensions, i.e. one inferior and one superior, as shown in Figs 3K, L and N ; and,

secondly, two others, as shown in Fig. 3M. Nevertheless, it is clear that both the last phenomena could happen simultaneously.

Where the paired setae *u* are concerned (Fig. 3P), they appear as leaf-like, denticulate phaneres, the shape of which is very similar to the ones shown in tarsi of the larva. The setae *u* are relatively longer in n1 than in both the other instars (e.g. length *u'*-length tarsus ratio is around 0.15 in n1 and around 0.13 in n2, n3 and also in Ad). This is another example indicating that the numerical inhibition of phaneres in leg IV of n1 does not act upon the size of the remaining setae (see above).

On the other hand, though the seta *u'* is always a bit broader than the seta *u''*, the breadth of setae *u* is appreciably greater in n3 than in n2 and n1 (e.g. breadth-length ratio of *u'n1* is around 0.50 in n3 and around 0.40 in the two other instars). In addition, in n3, the processes (usually five) join together more amply than in n2 and n1. The consequence is that, first, their tips are less distinct (note that it is more marked in *u'* than in *u''*), and second, the protective role of setae is all the better.

The setae *pv* are relatively short, rather thick and rectilinear phaneres which escape from the segment at a moderate, acute angle (the angle seems, however, a bit more marked in n1 than in both the other instars). Both the setae have appreciably the same thickness (the seta *pv'n1* was sometimes thicker than *pv''n1*) and, usually, the same number of barbels (i.e. four).

The shape of seta *sn2* is similar to the one of previous setae. There are also four, relatively thin and sharp barbels; consequently, the seta *sn2* is not ramose.

Finally, if all the dorsal setae of tarsus IV increase their relative length during ontogeny, it is quite the opposite among the ventral setae (*pv*) and (*u*) (e.g. the values of length *pv'*-length tarsus ratio are 0.18 in n1, 0.13 in n2, 0.15 in n3, but 0.19 in Ad; see above for the values shown by *u'*); but, not in *sn2* (length *s*-length tarsus ratio is around 0.14 in n2, around 0.22 in n3 and in Ad).

Though this relative decrease in length is always weak, it could be regarded as a precursory sign of regression (see GRANDJEAN, 1961, p. 209, for a general discussion). Note that: first, the protective

role of setae *u* can probably be regarded as a restraint on their complete disappearance in the near future; second, the strong decrease shown by the setae *dG* of larvae is undoubtedly such a sign, and refers to the phenomenon of "Rta" regression shown by this phanere in several genera (GRANDJEAN, 1942, p. 41).

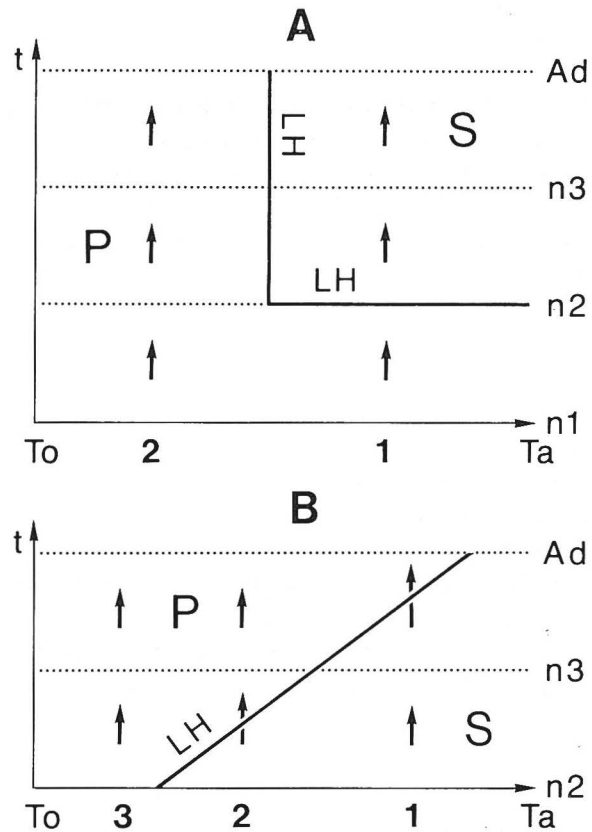


Fig. 4 : Ontophylogenetic diagrams showing PS (plesio-apomorphic) changes with their harmonic line (LH). — A : descendant harmony with stopping level at n2 shown by the relative length of setae *u* in tarsus IV (type IIID in GRANDJEAN, 1954, p. 421); P : relative length greater or equal to 0.15; S : relative length equal to 0.13; 1 : present time Ta at which the individuals of *T. maniculatus* spend their life (ontogenetic case O2, *loc. cit.*, p. 418); 2 : Ta at which the individuals of probably several other species of *Trimalaconothrus* spend their life (ontogenetic case O1). — B : ascendant harmony shown by the numerical regression of seta *ev'FIV* in Malaconothridae; 1 : present time Ta at which the species of *Malaconothrus* spend their life (ontogenetic case O3); 2 : Ta for the present species of *Trimalaconothrus* (same case); 3 : Ta for probably all the other species of oribatids (ontogenetic case O1).

Abbreviations. To : primitive time of the change PS in question; t : ontogenetic time.

As the decrease in length of setae *u* appears to be limited to n2, n3 and Ad, they concern a regression (the plesiomorphic state *P* is the size observed in n1; the apomorphic state *S* is the size shown in the three other instars; see annotation 3 at the end of the paper), the harmonic line of which is certainly vertical within an ontophylogenetic diagram (i.e., as shown in Fig. 4A, a line similar to the one of Fig. 6 in GRANDJEAN, 1954, p. 421, where  $N_i = n1$ ,  $N_r = n2$  and  $N_s = Ad$ ).

However, this does not seem to be the case of setae *pv* since a relative, substantial decrease in size is observed only in n2 and n3 (see annotation 4). Consequently, it is necessary to verify whether this regression in length either acts in other species of *Trimalaconothrus* or isolates *T. maniculatus* from all the other species of the genus.

#### Phaneres of other segments

In the trochanter, though the seta developing in n3 is very close to the plane of pseudosymmetry, we used the notation *v'* assuming thereby its homology with the setae appearing during ontogeny in leg IV of other oribatids (GRANDJEAN, 1946, p. 311). The seta is barbellate and strongly curved paraxially.

In the other, proximal segments, except the seta *dTn2* which is long, smooth and tactile, all the setae are barbellate (the most barbellate seta seeming to be *dF* in n2 as well in n3) and forward curved (the most curved seta is ever *dF*; the least is *v'T* in n2 and *dG* in n3).

In the femur, the seta *ev'* shows an ontogenetic retardation from n2 to n3 with respect to its homologues in other oribatids. As shown in Fig. 4B, this retardation refers to a harmonic line similar to the one of Fig. 3 in GRANDJEAN (1946, p. 311) where  $N_i = n2$  and  $N_s = Ad$  (see also annotation 5 in the next chapter).

Where the relative size of setae is concerned, one could admit that, from n2 to n3, both the setae *dG* and *dT* lengthen relatively more than both the setae *dF* and *v'T*.

Finally, the unguis appear as robust as in the larva. They show: first, proximal and minute ridges as well as very small barbs as observed in the larva using SEM; but, barbs and some few ridges are discernible at the scale of usual observation (note

that the lines depicting these ridges in Fig. 3F are certainly too thick); second, also as in the larva, a distal convexity along the inferior border; third, a slight, median hollow in the superior border; and, fourth, an antiaxial basculation (Fig. 3E). Note that in legs where the basculation of paired setae *p* and *u* was weak or absent, the basculation of the unguis was similarly less marked.

#### Evolutionary phenomena shown by phaneres

Figure 5 tries to summarize the main evolutionary facts shown by phaneres of leg IV in nymphs of *T. maniculatus*. There are, from trochanter to apotele: (1) Descent of the seta *v'R* in n3. (2) Curvature of the seta *dF* in n2 and n3. (3) Advance of the seta *ev'* in n3. (4) Ontogenetic retardation of the seta *ev'* (see also Fig. 4B and annotation 5). (5) Weak, prime shifting of the seta *dG* upon the genu in n2 and n3. (6) Lengthening of the seta *dT* in n2 and n3. (7) Shortening of setae (*pv*) in n2 and n3 (see also annotation 4). (8) Weak, prime disjunction of setae (*pv*) in n3. (9) Lengthening and thickening of the seta *ft''* in the three nymphs. (10) Shape of the seta *tc''* in n2 and n3. (11) Prime disjunction of setae (*tc*) in n2 and n3. (12) Weak, prime shifting of the seta *s* in n2 and n3. (13) Prime basculation of setae (*p*) and (*u*) in n1 and in some tarsi in n2 and n3. (14) Shape of the seta *p'* in the three nymphs and shape of the seta *p''* in n1 and n3 only. (15) Shape of setae (*u*) in the three nymphs. (16) Shortening of setae (*u*) in n2 and n3 (see also Fig. 4A and annotation 3). (17) Prime basculation of the unguis in all the nymphs.

As in the larva, the basculation of lyrifissures (but, only in n2 and n3) as well as the forward displacement of proximal setae upon the tarsus (to which the numerical regression of setae in n1 and the weak number of fundamental setae in n2 have obviously to be added) are also clear apomorphies shown by leg IV in nymphs.

#### CONCLUSIONS

Our conclusions will focus on three important remarks:

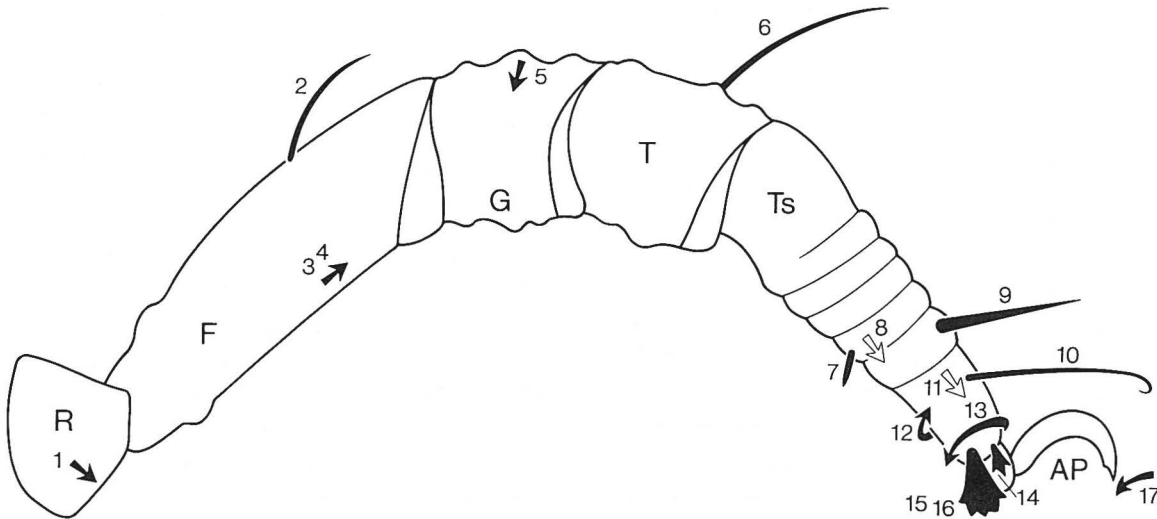


Fig. 5 — Schematic representation of the 17 main apomorphies shown by phaneres in leg IV of nymphs in *Trimalaconothrus maniculatus* Fain & Lambrechts. See the text for definitions of evolutionary phenomena outlined. Note and abbreviations as in Fig. 2.

1. The lack of eustasy shown by the seta *ev'n3* (the retardation of an usually eustasic phanere is uncommon, and seems always to be an indication of amphistasy ; see GRANDJEAN, 1964 c, p. 551 and annotation 5) appears to be a noticeable trait allowing the family of Malaconothridae to be clearly defined. Indeed, the priority (which refers to the strength by which setae resist to the phenomenon of numerical regression) of setae developing in n2 and n3 upon the proximal segments of leg IV is [*dF*, *dG*, *dT*, *v'T*], [*v'R*, *ev'F*] when, in other Nothroids (taking into account only the phaneres homologous to the ones shown in Malaconothridae), the priority should be [*dF*, *ev'F*, *dG*, *dT*, *v'T*], *v'R* (GRANDJEAN, 1946, p. 311-315).

Now, we know that a peculiar priority is a sufficient characteristic to define unambiguously a "true", phyletic branch within a given phylum (e.g. the one of Malaconothridae within oribatids ; see GRANDJEAN, 1964 c, p. 549).

2. The absence of any solenidion in leg IV reveals that *T. maniculatus*, as all the other Malaconothridae (GRANDJEAN, 1964 c, p. 531), has overshoot the second stage of detainment shown by Circumdehiscent oribatids since the solenidion that genera of these oribatids usually support is not present.

In the framework of the great numerical regression shown by solenidia in oribatids, the absence of

any solenidion in leg IV of Malaconothridae is a second major, apomorphic trait.

3. Whereas the presence of accessory setae belonging to "simple rows" is a common, plesiomorphic characteristic in many species of Nothroids (e.g., in *Platynothis peltifer*, 6 simple rows are observed in leg IV : 2 in the femur, and 4 in the tarsus ; GRANDJEAN, 1972, p. 464), the lack of such rows in *T. maniculatus* as well as in other species of *Trimalaconothrus* (see e.g. Fig. 4 in KNÜLLE, 1957, p. 192) is a third patent, apomorphic trait.

However, in the second part of this study, we will point out the presence of several accessory setae on the other legs of nymphs, and we will discuss their origin.

#### ANNOTATIONS

1. In oribatids, in which the primiventral setae or the antelateral ones have disappeared, the taxic notation of setae remaining ventrally on tarsi is quite unclear (GRANDJEAN, 1941, p. 38).

In the case of the two ventroproximal setae present on tarsi in the larva of *T. maniculatus*, J. TRAVÉ (*in litt.*) suggests five possible notations as follows. (1) The two phaneres are the primiventral setae (i.e. *pv'* and *pv''*) which, like the dorsal phaneres, have moved forward upon the segment.

This means that the setae  $s$ ,  $a'$  and  $a''$  are removed from the normal, fundamental type of chaetotaxy showing 13 setae in oribatids (see GRANDJEAN, 1941, p. 36). (2) The two setae are the antelateral ones (i.e.  $a'$  and  $a''$ ). Consequently, the setae  $s$  and ( $pv$ ) have disappeared. (3) Or, the notation is a mixture of both the previous ones (i.e.  $pv'$  and  $a''$ , or  $a'$  and  $pv''$ ). (4) The two setae which remain ventrally on tarsi are  $s$  and  $a'$ , respectively. (5) Or, finally, they are  $s$  and  $pv'$ . In addition, the setae in question are under no obligation to receive the same notation in the three tarsi.

Any of these designations appears to be reasonably good. Indeed, assuming notations 1-3, we must admit the deficiency of seta  $s$ , and this seems quite uncommon (GRANDJEAN, 1941, p. 39). Assuming notation 4, a location of the seta  $s$  in front of  $a'$  is observed in tarsus I; and, this would be the case only if the seta  $s$  were an eupathidium (see e.g. GRANDJEAN, 1959 b, p. 462). Assuming notation 5, a location of the seta  $pv'$  in front of  $s$  would be registered; but, such a displacement of  $pv'$  in a forward direction has never been observed in oribatids, even in species where  $pv''$  has disappeared and the number of fundamental setae is few (see e.g. the case of *Mucronothrus nasalis*, a species close to those of *Trimalacothonrus*, studied by TRAVÉ, 1971).

Our assumption that, in *T. maniculatus*, the ventroproximal setae developed on all the tarsi are metahomologous and must be called ( $pv$ ) is supported by two (slight) arguments.

The first argument refers to the similarity of both the form (but, as stated above, this contravenes the rule of metameric reinforcement) and the prime disjunction (but, in tarsus IV, in n3 and Ad only) shown by the ventroproximal setae, both on the tarsus III of larvae and on the tarsus IV of nymphs (note that, in the tarsus IV of n1, the setae in question are indubitably the primiventral ones). The second argument refers to the similarity of location shown in the larva by these setae, both on the tarsus II and on the two other tarsi.

2. Our further investigations will indicate that, in leg III of nymphs, there is also a prime (antiaxial) disjunction of paired setae  $tc$  whereas, in legs I and II, the disjunction is double prime (i.e. likewise antiaxial).

Because the disjunctions shown by nymphs are antiaxial in all the legs, the longitudinal shiftings both of the seta  $tc'$  in tarsi III-IV and the seta  $tc''$  in tarsi I-II may be regarded as apomorphies not consistent with RPH (i.e. likely adaptative evolutions; see GRANDJEAN, 1961, p. 212 for a discussion).

On the other hand, though the shape of these setae is quite different from the one of their metahomologues on legs I-III in the larva, the notation we used is undoubtedly  $tc$  (and not  $it$ ) because the setae in question appear in n2. Indeed, in leg IV, only setae  $tc$  may develop dorsally in n2, between  $ft''$  and the setae ( $p$ ) since the  $tc$  are fundamental, eustasic setae (with few exceptions; see GRANDJEAN, 1964 b, p. 180). On the contrary, because the setae  $it$  are amphistasic, they either develop at a higher level of ontogeny than n2 (i.e. in n3 or in Ad) or they show a complete regression as apparently in all the Malaconothridae, the development of which is known (GRANDJEAN, 1964 b, p. 179).

3. Where the decrease in length of setae  $u$  is concerned, we assume that: first, the time  $T_0$  of the regression (i.e. its primary time) refers to the time at which, in the ancestors of present n2, n3 and Ad, the length of setae  $u$  was the one observed in present n1; second, this length has been gained by a previous decrease older than the one to which Fig. 4A refers, and acting upon all the stases.

This means that the plesiomorphic state of the decrease in length depicted in Fig. 4A is itself the apomorphic state of a former decrease; but, at the present, we don't know species of *Trimalacothonrus* affected by this old phenomenon. Therefore, from a phylogenetic standpoint, the acquiring of a smaller length may be regarded as a "novelty" *sensu* GRANDJEAN (1954, p. 418).

4. In the case of the shortening shown by the setae  $pv$ , the ontophylogenetic diagram would be a mixture of both Figs 6 and 8 in GRANDJEAN (1954, p. 421).

Indeed, the plesiomorphic state P of the regression (i.e. a relative length greater or equal to 0.18) is achieved both in n1 and Ad whereas the apomorphic state S (i.e. a relative length lower or equal to 0.15) is observed in n2 and n3. This means that

such a regression in length is not phylogenetically concordant, and that the corresponding line of evolution cannot be regarded as harmonic because the change *PS* occurs twice during ontogeny (GRANDJEAN, 1954, p. 419).

5. We may also hypothesize that the retardation of the seta *ev'n3* is not an indication of amphistasy; but, that the seta, in its regressive evolution, has temporarily stopped at an eustasic stage.

To have proved this hypothesis, presence/absence variations of this seta should have been observed in tritonymphs of the population studied. Then, in the case of eustasy, adults of this population should have or should not have the seta (in both the legs IV or only in one, on the left or on the right side) whereas, in the case of amphistasy, all the adults should have *ev'n3*. Unfortunately, no such variations were registered. The study of other species will probably solve the problem.

However, the fact that *ev'* appears only in adults in the genus *Malaconothrus* seems to be a strong argument to assume the amphistasy of this seta in the family of Malaconothridae (Fig. 4B).

#### ACKNOWLEDGEMENTS

For comments, suggestions and advice on our study, we are indebted to Dr. J. TRAVÉ (Laboratoire Arago, Banyuls-sur-Mer), Dr. P. GROOTAERT and Dr. G. COULON (I.R.Sc.N.B., Brussels). As usual, thanks are extended to Mr. R.D. KIME for reviewing our english manuscript. Thanks are also due to Mrs. I. SAUVAGE and Mr. H. VAN PAESSCHEN for their valuable assistance.

#### REFERENCES

- FAIN (A.) & LAMBRECHTS (L.), 1987 — Observations on the acarofauna of fish aquariums. II. A new oribatid and two new halacarid mites. — Bull. Anns Soc. r. belge Ent., **123** : 103-118.
- GRANDJEAN (F.), 1933 — Etude sur le développement des Oribates. — Bull. Soc. zool. France, **58** : 30-61.
- Grandjean (F.), 1940 a — Observations sur les Oribates (13<sup>e</sup> série). — Bull. Mus. nat. Hist. natur., **12** : 62-69.
- GRANDJEAN (F.), 1940 b — Les poils et les organes sensitifs portés par les pattes et le palpe chez Oribates. Deuxième partie. — Bull. Soc. zool. France, **45** : 32-44.
- GRANDJEAN (F.), 1941 — La chaetotaxie comparée des pattes chez les Oribates (1<sup>re</sup> série). — Bull. Soc. zool. France, **66** : 33-50.
- GRANDJEAN (F.), 1942 — La chaetotaxie comparée des pattes chez les Oribates (2<sup>e</sup> série). — Bull. Soc. zool. France, **67** : 40-53.
- GRANDJEAN (F.), 1946 — La signification évolutive de quelques caractères des Acariens. — Bull. biol. France Belg., **79** : 297-325.
- GRANDJEAN (F.), 1947 a — Observations sur les Oribates (17<sup>e</sup> série). — Bull. Mus. nat. Hist. natur., **19** : 165-172.
- GRANDJEAN (F.), 1947 b — Etude sur les Smarididae et quelques autres Érythroïdes. — Arch. Zool. exp. gén., **85** : 1-126.
- GRANDJEAN (F.), 1954 — Les deux sortes de temps et l'évolution. — Bull. biol. France Belg., **88** : 413-434.
- GRANDJEAN (F.), 1959 a — *Hammation sollertius* n.g., n.sp. (Acarien, Oribate). — Mém. Mus. nat. Hist. natur., sér. A, Zool., **16** : 173-198.
- GRANDJEAN (F.), 1959 b — Sur le genre *Mochlozetes* GRANDJ. 1930. — Acarologia, **1** : 452-474.
- GRANDJEAN (F.), 1960 a — *Damaeus arvernensis* n.sp. (Oribate). — Acarologia, **2** : 250-275.
- GRANDJEAN (F.), 1960 b — Les *Mochlozetidae* n. fam. (Oribates). — Acarologia, **2** : 101-148.
- GRANDJEAN (F.), 1961 — Nouvelles observations sur les Oribates (1<sup>re</sup> série). — Acarologia, **3** : 206-231.
- GRANDJEAN (F.), 1962 a — Le genre *Tegeocranellus* BERL. 1913. — Acarologia, **4** : 78-100.
- GRANDJEAN (F.), 1962 b — Au sujet des Hermanniellidae (Oribates). Deuxième partie. — Acarologia, **4** : 632-670.
- GRANDJEAN (F.), 1964 a — *Pheroliodes wehnckeii* (WILLMANN) (Oribate). — Acarologia, **6** : 353-386.
- GRANDJEAN (F.), 1964 b — Nouvelles observations sur les Oribates (3<sup>e</sup> série). — Acarologia, **6** : 170-198.
- GRANDJEAN (F.), 1964 c — La solénidiotaxie des Oribates. — Acarologia, **6** : 529-556.
- GRANDJEAN (F.), 1972 — Caractères anormaux et verticillaires rencontrés dans des clones de *Platynothrus peltifer* (KOCH). Chapitres I à VI de la deuxième partie. — Acarologia, **14** : 454-478.
- HAMMEN (L., van der), 1977 — A new classification of Chelicerata. — Zool. Meded. Leiden, **51** : 307-319.
- HAMMEN (L., van der) 1980 — Glossary of acarological terminology. Vol. 1. General terminology.— Dr. W. Junk, The Hague, 244 pp.
- KNÜLLE (W.), 1957 — Morphologische und entwicklungs-geschichtliche Untersuchungen zum phylogenetischen System der Acari : Acariformes ZACHV. I. Oribatei : Malaconothridae. — Mitt. Zool. Mus. Berlin, **33** : 97-213.

SHULTZ (J.W.), 1989 — Morphology of locomotor appendages in Arachnida : evolutionnary trends and phylogenetic implications. — Zoological Journal of the Linnean Society, 97 : 1-56.

TRAVÉ (J.), 1971 — The specific stability and the chaetotactic variations in *Mucronothrus nasalis* WILLM. (Oribatei). — Proc. 3rd Int. Congr. Acarology Prague 1971 : 303-309.

*Paru en Décembre 1991.*

---